NASA Technical Memorandum 81348

COMPARISON OF STRUCTURAL BEHAVIOR OF SUPERPLASTICALLY FORMED/DIFFUSION-BONDED SANDWICH STRUCTURES AND HONEYCOMB CORE SANDWICH STRUCTURES

William L. Ko

June 1980

NASA Technical Memorandum 81348

COMPARISON OF STRUCTURAL BEHAVIOR OF SUPERPLASTICALLY FORMED/DIFFUSION-BONDED SANDWICH STRUCTURES AND HONEYCOMB CORE SANDWICH STRUCTURES

William L. Ko
Dryden Flight Research Center
Edwards, California

National Aeronautics and
Space Administration
1980

COMPARISON OF STRUCTURAL BEHAVIOR OF SUPERPLASTICALLY FORMED/DIFFUSION-BONDED SANDWICH STRUCTURES AND HONEYCOMB CORE SANDWICH STRUCTURES

William L. Ko
Dryden Flight Research Center

INTRODUCTION

For years the honeycomb core sandwich structure has enjoyed popularity in aerospace applications because of its extremely high structural efficiency (that is, light weight and high stiffness). Since the stiffness (that is, bending, transverse shear, and so forth) and stability of this structure depend strongly on the geometry of the honeycomb cell, there have been constant improvements in the manufacturing process to optimize honeycomb cell geometry.

In general, this type of sandwich structure is constructed by bonding the honeycomb core between two face sheets by using a bonding agent. Because the honeycomb core wall is quite thin, the bonding contact between the honeycomb core and the face sheets is practically a line contact. This is a major shortcoming of this type of sandwich structure because the line contact bonded joints are subject to damage due to corrosion during the structure's service life.

Another type of sandwich structure which has emerged in recent years and may compete with the conventional honeycomb core sandwich structure is the so-called superplastically formed/diffusion-bonded (SPF/DB) sandwich structure using superplastic alloys such as titanium. Since titanium is used, this new sandwich structure is a good candidate for structural components that are constantly exposed to elevated temperature environments (such as supersonic cruise conditions). Detailed discussions of SPF/DB technology are to be found in references 1 to 3.

In the SPF/DB sandwich structure, the face sheets and the sandwich core are solid state diffusion bonded without the use of a bonding agent. Thus, the corrosion damage problems at the bonding joints are completely eliminated. Another feature of this new sandwich structure is that the bonding contact region between the surface sheets and the sandwich core is surface contact rather than line contact.

Using the SPF/DB technique, a wide variety of sandwich core geometries becomes possible (truss cores, sinusoidal cores, dimpled cores, and so forth (ref. 1)). A high efficiency core geometry created by the author is the so-called SPF/DB orthogonally corrugated core sandwich structure (ref. 4). This is one of the high-stiffness sandwich structures which could easily be generated by using the SPF/DB process.

The purpose of this report is to describe this new sandwich structure and to discuss the structural characteristics of this new structure relative to the conventional honeycomb core sandwich structure.

SYMBOLS

a	length of sandwich plate
c	width of sandwich plate
D_c	$= \frac{1}{12} E_c h_c^3$, bending stiffness, per unit width, of a solid beam with depth h_c, made of material with Young's modulus E_c
$\tilde{D}_c$	$= \frac{1}{12} E_c \tilde{h}^3$, same definition as above except that h_c is replaced by $\tilde{h}$
D_{Q_x}, D_{Q_y}	transverse shear stiffnesses, per unit width, of beams cut from sandwich plate respectively in x- and y-directions
D_x, D_y	bending stiffnesses, per unit width, of beams cut from sandwich plate respectively in x- and y-directions
D_x^*, D_y^*	bending stiffnesses, per unit width, of beams cut from SPF/DB orthogonally corrugated core respectively in x- and y-directions
D_{xy}	twisting stiffness of unit-width and unit-length element cut from sandwich plate with edges parallel to x- and y-axes
$\tilde{D}_y$, $\tilde{D}_z$	bending stiffnesses, per unit width, of beams cut from honeycomb core respectively in y- and z-directions

$\tilde{D}_{\bar{y}}$, $\tilde{D}_{\bar{z}}$	bending stiffnesses, per unit width, of beams cut from square-cell core respectively in $\bar{y}$- and $\bar{z}$-directions
E_c	Young's modulus of sandwich core material
E_s	Young's modulus of sandwich face sheet material ($E_s = E_c$)
E_x	effective Young's modulus in thickness direction of honeycomb core
E_z^*	effective Young's modulus in thickness direction of SPF/DB orthogonally corrugated core
f	length of flat segment (crest or trough) of corrugation leg
G_c	shear modulus of sandwich core material
G_{xy}^*, G_{yz}^*, G_{zx}^*	effective shear moduli for SPF/DB orthogonally corrugated core respectively in xy-, yz-, and zx-planes
$G_{x\bar{y}}$, $G_{\bar{z}x}$	effective shear moduli for square-cell core respectively in $x\bar{y}$- and $\bar{z}x$-planes
h	thickness of sandwich plate (distance between middle surfaces of two face sheets)
h_c	corrugated core thickness (vertical distance between upper and lower corrugation flat segments' middle surfaces)
$\tilde{h}$	honeycomb core thickness
$\tilde{I}_c$	moment of inertia, per unit width, of square-cell core cross section (normal to vertical wall axis) taken about the horizontal centroidal axis of the cross section
I_s	$= \frac{1}{2}t_s h^2$, moment of inertia, per unit width, of face sheets (considered as membranes) taken about sandwich plate middle surface
ℓ	length of one corrugation leg
m	number of buckle half-waves in sandwich plate in x-direction

N_x	longitudinal compressive buckling load, per unit width, of sandwich plate
n	number of buckle half-waves in sandwich plate in y-direction
p	one-half of corrugation pitch (or one-half wave length of corrugation)
R	radius of circular arc segments of corrugation leg
t_c	$= \frac{p - f}{\ell - f} t_f$, thickness of circular arc segments or of straight diagonal segment of corrugation leg
t_f	thickness of corrugation leg flat segments (original core sheet's thickness before superplastic expansion)
t_s	thickness of sandwich face sheets
x, y, z	rectangular Cartesian coordinates (figs. 3, 10, 14)
x, $\bar{y}$, $\bar{z}$	rectangular Cartesian coordinates for square-cell core (fig. 14)
$[]_{HC}$	quantity associated with honeycomb core
$[]_{SC}$	quantity associated with square-cell core
$[]_{SP}$	quantity associated with SPF/DB orthogonally corrugated core
γ	density of sandwich core
θ	corrugation angle
ν_c	Poisson ratio of sandwich core material
ν_s	Poisson ratio of sandwich face sheet ($\nu_s = \nu_c$)

ORTHOGONALLY CORRUGATED CORE SANDWICH PANEL

Figure 1 shows the four superplastic alloy sheets (two face sheets and two core sheets) needed for fabricating an orthogonally

corrugated core sandwich panel by using SPF/DB technique. The interfacial bonding region between the top face sheet and the upper core sheet is a square mesh of narrow bonding strips. The interfacial bonding region between the upper and the lower core sheets is a finer square mesh of narrow bonding strips which lie vertically below the diagonals of the square mesh of the upper core sheet. Thus, the length of one side of a unit square of the mesh on the lower core sheet is one-half the diagonal length of a unit square of the mesh on the upper core surface. Finally, the bonding region between the lower core sheet and the bottom face sheet is similar to that on the upper core sheet except that the former is shifted relative to the latter in the diagonal direction by a distance of half of the diagonal length of a unit square of the mesh.

During diffusion bonding, the square strip A'B'C'D' on the upper surface of the upper core sheet will be bonded to a square strip region ABCD lying on the bottom surface of the top face sheet. The diagonal strips EB'G and FB'H lying on the lower surface of the upper core sheet will be bonded respectively to the strip regions E'B"G' and F'B"H' lying on the upper surface of the lower core sheet. Finally, the square strip E'F'G'H' lying on the lower face of the lower core sheet will be bonded to the square strip region E"F"G"H" lying on the upper face of the bottom face sheet. The arrows shown at typical points indicate the directions of movement of those points during the superplastic expansion process.

In the upper and lower core sheets, an array of pressure-gas-passing holes is provided for gas pressure to penetrate to each core cell compartment to ensure the proper expansion of the diffusion-bonded sheet pack. Figure 2 shows the familiar SPF/DB process for the four-component sheet pack.

At the end of superplastic expansion, the upper core sheet is deformed to form an array of inverted hollow pyramids, and the lower core sheet an array of upright hollow pyramids. These two sets of pyramids are bonded together at the edges of their triangular sides to form an orthogonal corrugation. Figure 3 shows the final configuration of the orthogonally corrugated core sandwich panel. This new structure is far superior to the ordinary SPF/DB unidirectionally corrugated core sandwich structure and is one of the high-efficiency structures which could be generated by using SPF/DB technique.

ELASTIC CONSTANTS FOR SPF/DB ORTHOGONALLY CORRUGATED SANDWICH CORE

For stiffness, stability, and vibration analyses of a sandwich structure, knowledge of the effective elastic constants for the sandwich core is needed. Effective elastic constants for SPF/DB unidirectionally corrugated sandwich core (fig. 4) were calculated by Ko and are presented in reference 5. The results of this work can then be used to construct most of the effective elastic constants for SPF/DB orthogonally corrugated sandwich core. The calculations of all the elastic constants for this sandwich core appear in reference 6. The four major elastic constants of this sandwich structure, E_z^* (thickness stiffness), G_{xy}^* (shear modulus in the xy-plane), $G_{yz}^* = G_{zx}^*$ (shear modulus in yz- or zx-plane), and $D_x^* = D_y^*$ (bending stiffness in x- or y-direction) are plotted against p/h_c (dimensionless half corrugation pitch) respectively in figures 5, 6, 7, and 8, with t_f/h_c (dimensionless initial core sheet thickness) and θ (corrugation angle) as parameters. In these plots, R (the radius of the circular arc segments of the corrugation leg) was set equal to t_f. From these figures we observe the following facts:

(1) For any given values of t_f and θ, the triangularly corrugated core (that is, zero crest length or f = 0) has the highest values of the thickness stiffness E_z^* and the transverse shear stiffness G_{yz}^*. For this particular core, the values of E_z^* and G_{yz}^* reach their maximum values respectively near $\theta = 65°$ and $\theta = 55°$. The reason the value of E_z^* decreases at large values of θ (greater than, say, $\theta = 70°$) is that the core wall becomes too thin after superplastic expansion.

(2) Both E_z^* and G_{yz}^* are quite sensitive to changes in the value of p (or f). Specifically, a slight increase in the value of f from f = 0 will drastically reduce the values of both E_z^* and G_{yz}^*.

(3) For any given values of t_f and θ, the triangularly corrugated core (that is, f = 0) has the lowest values of

the in-plane shear stiffness G^*_{xy} and the bending stiffness D^*_x (or D^*_y). This is expected, because for a finite value of f, the crest regions will contribute a certain resistance in in-plane shear and bending.

(4) Because the behavior of D^*_x (or D^*_y) and G^*_{xy} with respect to f is opposite to the behavior of E^*_z and G^*_{yz}, care must be exercised in optimizing the overall structural properties of the new sandwich structure.

Figure 9 shows the above four elastic constants plotted for a right triangularly corrugated core (that is, f = 0, $\theta = 60°$). This figure will be used in a comparison of the structural behavior of this particular core and the conventional honeycomb core or a square-cell core (optimum state of honeycomb core).

HONEYCOMB SANDWICH CORE

As shown in figure 10, the conventional honeycomb core is made up of numerous corrugated strips which are joined together at their crests and troughs. Thus, the formulae for evaluating the elastic constants (except for bending stiffness) for the SPF/DB unidirectionally corrugated core reported in reference 5 may be used to calculate elastic constants for the honeycomb core if the coordinate system is properly chosen (fig. 10) and if t_c is set equal to t_f.

A typical honeycomb core which is used in high speed aircraft has the following geometric parameters: $\frac{t_f}{h_c} = 0.0147$, $\frac{f}{h_c} = 0.4053$, $\frac{p}{h_c} = 0.9825$, $\frac{\ell}{h_c} = 1.5600$, and $\theta = 60°$.

Plots of elastic constants (thickness stiffness, E_x; transverse shear stiffness, G_{xy} and G_{zx}; and bending stiffness, $\tilde{D}_y$ and $\tilde{D}_z$) for a honeycomb core with the above geometric parameters are shown in figures 11, 12, and 13 (refs. 5 and 6). In these plots both R and t_c were set equal to t_f. Figures 12 and 13 were plotted for f = 0 because $\tilde{D}_y$ and $\tilde{D}_z$ are practically independent of f.

The bending stiffness of an ordinary honeycomb (hexagonal cell) core ($f \neq 0$, fig. 10) varies with the direction of bending, and the peak value is not the highest attainable peak value for sandwich cores of the same core density and material. If the hexagonal cell honeycomb core is reduced to a square-cell core (see fig. 14) by making $f = 0$ and $\theta = \frac{\pi}{4}$, then the new core will consist of two families of straight-through vertical walls which will intersect each other at 90° and will have the highest attainable peak bending stiffnesses in both the $\bar{y}$- and $\bar{z}$-directions (with the same core density and material).

For this square-cell core, the bending stiffness $\tilde{D}_{\bar{y}}$ (or $\tilde{D}_{\bar{z}}$) in the $\bar{y}$- or $\bar{z}$-direction may be expressed as

$$\tilde{D}_{\bar{y}} = \tilde{D}_{\bar{z}} = E_c \tilde{I}_c \tag{1}$$

where

$$\tilde{I}_c = \frac{t_c h^3}{12\ell} \; ; \; \ell = \sqrt{2\, h_c} \tag{2}$$

and the transverse shear stiffness $G_{x\bar{y}}$ (or $G_{x\bar{z}}$) in the $x\bar{y}$-plane or in the $x\bar{z}$-plane may be written as

$$G_{x\bar{y}} = G_{x\bar{z}} = G_c \frac{t_c}{\ell}; \; \ell = \sqrt{2\, h_c} \tag{3}$$

COMPARISON OF SANDWICH CORES

In the following comparison of the structural properties of the SPF/DB orthogonally corrugated sandwich core and the honeycomb core, it will be assumed that both types of sandwich cores have the same core density and core thickness.

The density of the SPF/DB orthogonally corrugated core γ_{SP} may be written

$$\gamma_{SP} = 2 \left[\frac{t_f}{h_c} \right]_{SP} \gamma_{Ti} \tag{4}$$

and the density of a honeycomb core γ_{HC} may be expressed as

$$\gamma_{HC} = \left[\frac{t_f \ell}{h_c p}\right]_{HC} \gamma_c \qquad (5)$$

where for an aluminum honeycomb core $\gamma_c = \gamma_{Al}$, and for a titanium honeycomb core $\gamma_c = \gamma_{Ti}$.

For the square-cell core, equation (5) can be reduced to

$$\gamma_{HC}\Big|_{\substack{f=0 \\ \theta=\frac{\pi}{4}}} = \gamma_{SC} = \sqrt{2}\left[\frac{t_f}{h_c}\right]_{SC}\gamma_c \qquad (6)$$

If γ_{HC} (eq. (5)) represents the core density of the typical honeycomb core having the geometric parameters given earlier, then under conditions of equal core density ($\gamma_{SP} = \gamma_{SC} = \gamma_{HC}$), equations (4) and (6) may be used to find the core sheet thickness $[t_f/h_c]_{SP}$ and $[t_f/h_c]_{SC}$, respectively for the SPF/DB orthogonally corrugated core and the square-cell core.

The results are summarized in table 1.

TABLE 1.- CORE WALL THICKNESSES OF EQUAL-DENSITY SANDWICH CORES ($\gamma_{SP} = \gamma_{SC} = \gamma_{HC}$)

	GIVEN HONEYCOMB CORE	SQUARE-CELL CORE	SPF/DB ORTHOGONALLY CORRUGATED CORE	
			HONEYCOMB CORE-ALUMINUM	HONEYCOMB CORE-TITANIUM
$\frac{t_f}{h_c}$	0.0147	0.0165	0.0073	0.0117

COMPARISON OF STIFFNESSES

Based on the values of t_f/h_c in table 1, appropriate values of elastic constants for the SPF/DB orthogonally corrugated core and the honeycomb core may be found, respectively, from figure 9 and figures 11 to 13. For the square-cell core, the elastic constants may be calculated from equations (1) and (3).

Tables 2 and 3 show comparisons of the elastic constants for the honeycomb core, square-cell core, and the SPF/DB orthogonally corrugated core, all of which have the same core density ($\gamma_{SP} = \gamma_{SC} = \gamma_{HC}$). In table 1, both the honeycomb and the square-cell cores are made of aluminum, while in table 2 they are made of titanium. Note that the elastic constants for the square-cell core are associated with the $x, \bar{y}, \bar{z}$-system rather than the x, y, z-system. The bending stiffnesses for all of the sandwich cores were calculated under conditions of equal core thickness. In the calculations of $\tilde{D}_y$ and $\tilde{D}_z$ for the honeycomb core, the constraint effect of the surface sheets was taken into account (ref. 6). For the other two types of cores (that is, SPF/DB orthogonally corrugated core and square-cell core), the core bending stiffnesses are insensitive to the existence of the surface sheets.

From tables 2 and 3, we observe that the SPF/DB orthogonally corrugated core has lower thickness stiffness (is softer) than the other two types of sandwich cores, which are made of aluminum or titanium. Except for thickness stiffness, the SPF/DB orthogonally corrugated core is stiffer than either the typical honeycomb core made of aluminum or titanium or the aluminum square-cell core. However, if the square-cell core is made of titanium, it is slightly stiffer in every respect than the SPF/DB orthogonally corrugated core.

TABLE 2. - COMPARISON OF ELASTIC CONSTANTS FOR ALUMINUM HONEYCOMB CORE, ALUMINUM SQUARE-CELL CORE, AND SPF/DB TITANIUM ORTHOGONALLY CORRUGATED CORE

ALUMINUM HONEYCOMB CORE	ALUMINUM SQUARE-CELL CORE	SPF/DB TITANIUM ORTHOGONALLY CORRUGATED CORE	$\frac{\Pi_{SP}}{\Pi_{HC}}$	$\frac{\Pi_{SP}}{\Pi_{SC}}$
$\frac{t_f}{h_c} = 0.0147$, $\frac{f}{h_c} = 0.4053$, $\theta = 60°$, $\tilde{h} = 2.54 \times 10^{-2}$ m (1 in.)	$\frac{t_f}{h_c} = 0.0165$, $f = 0'$ $\theta = 45°$, $\tilde{h} = 2.54 \times 10^{-2}$ m (1 in.)	$\frac{t_f}{h_c} = 0.0073$, $f = 0$, $\theta = 60°$, $h_c = 2.54 \times 10^{-2}$ m (1 in.)	----	----
$E_x = 14.48 \times 10^8$ N/m^2 (21.00×10^4 psi)	$E_x = 14.48 \times 10^8$ N/m^2 (21.00×10^4 psi)	$E_z^* = 9.27 \times 10^8$ N/m^2 (13.44×10^4 psi)	0.64	0.64
$G_{xy} = 2.48 \times 10^8$ N/m^2 (3.60×10^4 psi)	$G_{x\bar{y}} = 3.22 \times 10^8$ N/m^2 (4.67×10^4 psi)	$G_{yz}^* = 3.25 \times 10^8$ N/m^2 (4.71×10^4 psi)	1.31	1.01
$G_{zx} = 2.59 \times 10^8$ N/m^2 (3.76×10^4 psi)	$G_{\bar{z}x} = 3.22 \times 10^8$ N/m^2 (4.67×10^4 psi)	$G_{zx}^* = 3.25 \times 10^8$ N/m^2 (4.71×10^4 psi)	1.25	1.01
$\tilde{D}_y = 1.69 \times 10^2$ N-m (1.50×10^3 in-lb)	$D_{\bar{y}} = 10.99 \times 10^2$ N-m (9.72×10^3 in-lb)	$D_x^* = 12.05 \times 10^2$ N-m (10.67×10^3 in-lb)	7.13	1.10
$\tilde{D}_z = 15.25 \times 10^2$ N-m (13.50×10^3 in-lb)	$D_{\bar{z}} = 10.99 \times 10^2$ N-m (9.72×10^3 in-lb)	$D_y^* = 12.05 \times 10^2$ N-m (10.67×10^3 in-lb)	0.79	1.10

TABLE 3. - COMPARISON OF ELASTIC CONSTANTS FOR TITANIUM HONEYCOMB CORE, TITANIUM SQUARE-CELL CORE, AND SPF/DB TITANIUM ORTHOGONALLY CORRUGATED CORE

TITANIUM HONEYCOMB CORE	TITANIUM SQUARE-CELL CORE	SPF/DB TITANIUM ORTHOGONALLY CORRUGATED CORE	$\frac{\Pi_{SP}}{\Pi_{HC}}$	$\frac{\Pi_{SP}}{\Pi_{SC}}$
$\frac{t_f}{h_c} = 0.0147$, $\frac{f}{h_c} = 0.4053$, $\theta = 60°$, $\tilde{h} = 2.54 \times 10^{-2}$ m (1 in.)	$\frac{t_f}{h_c} = 0.0165$, $f = 0$, $\theta = 45°$, $\tilde{h} = 2.54 \times 10^{-2}$ m (1 in.)	$\frac{t_f}{h_c} = 0.0117$, $f = 0$, $\theta = 60°$, $h_c = 2.54 \times 10^{-2}$ m (1 in.)	----	----
$E_x = 23.17 \times 10^8$ N/m^2 (33.60×10^4 psi)	$E_x = 23.17 \times 10^8$ N/m^2 (33.60×10^4 psi)	$E_z^* = 13.20 \times 10^8$ N/m^2 (19.20×10^4 psi)	0.57	0.57
$G_{xy} = 3.85 \times 10^8$ N/m^2 (5.58×10^4 psi)	$G_{x\bar{y}} = 4.99 \times 10^8$ N/m^2 (7.23×10^4 psi)	$G_{yz}^* = 4.39 \times 10^8$ N/m^2 (6.37×10^4 psi)	1.14	0.88
$G_{zx} = 4.02 \times 10^8$ N/m^2 (5.83×10^4 psi)	$G_{\bar{z}x} = 4.99 \times 10^8$ N/m^2 (7.23×10^4 psi)	$G_{zx}^* = 4.39 \times 10^8$ N/m^2 (6.37×10^4 psi)	1.09	0.88
$\tilde{D}_y = 2.71 \times 10^2$ N-m (2.40×10^3 in-lb)	$D_{\bar{y}} = 17.58 \times 10^2$ N-m (15.56×10^3 in-lb)	$D_x^* = 17.02 \times 10^2$ N-m (15.07×10^3 in-lb)	6.28	0.97
$\tilde{D}_z = 24.41 \times 10^2$ N-m (21.60×10^3 in-lb)	$D_{\bar{z}} = 17.58 \times 10^2$ N-m (15.56×10^3 in-lb)	$D_y^* = 17.02 \times 10^2$ N-m (15.07×10^3 in-lb)	0.70	0.97

COMPARISON OF BUCKLING BEHAVIOR

Figure 15 shows the geometry of three types of simply supported rectangular sandwich plates (with, respectively, SPF/DB orthogonally corrugated core, square-cell core, and SPF/DB unidirectionally corrugated core) for a buckling study. Using the formulae developed in reference 7, buckling curves for the above three types of sandwich plates may be obtained. Notice that in the buckling study, the coordinate system used for the square-cell core sandwich plate is different from that used in figure 14.

For obtaining the buckling curves for the square-cell core sandwich plate, the following expressions were used in the buckling equation given in reference 7:

$$D_x = D_y = E_c\tilde{I}_c + E_sI_s \tag{7}$$

$$D_{xy} = \frac{E_sI_s}{1 + \nu_c} \tag{8}$$

$$D_{Q_x} = D_{Q_y} = G_c\frac{t_ch}{\ell} \tag{9}$$

The buckling curves shown in figures 16 and 17 are for equal sandwich density, equal sandwich core depth and $c/h_c = 20$, $n = 1$, $E_s = E_c$, $\nu_s = \nu_c$. When the square-cell core sandwich plate is made of aluminum (fig. 16), the SPF/DB orthogonally corrugated core sandwich plate can carry a slightly higher buckling load than the square-cell core sandwich plate. If titanium is used for the square-cell core sandwich plate (fig. 17), it becomes slightly stronger in buckling than the SPF/DB orthogonally corrugated core sandwich plate. One also notices from figures 16 and 17 that the SPF/DB unidirectionally corrugated core sandwich plate has the lowest buckling resistance of the three types of sandwich plates studied.

CONCLUDING REMARKS

A new type of SPF/DB orthogonally corrugated core sandwich structure fabricated from four component sheets was discussed in detail.

Under the condition of equal structural density, the stiffness and buckling characteristics of this new sandwich structure were compared with those of honeycomb core sandwich structure, square-cell core sandwich structure, and SPF/DB unidirectionally corrugated core sandwich structure.

It was found that the new SPF/DB orthogonally corrugated core sandwich structure has structural efficiency comparable to that of the square-cell core sandwich structure (the optimum form of honeycomb core sandwich structure).

Dryden Flight Research Center
National Aeronautics and Space Administration
Edwards, California, April 8, 1980

REFERENCES

1. Pulley, John: Evaluation of Low-Cost Titanium Structure for Advanced Aircraft. NASA CR-145111, 1976.

2. Weisert, E. D.; Stacher, G. W.; and Kim, B. W.: Manufacturing Methods for Superplastic Forming/Diffusion Bonding Process. AFML-TR-79-4053, Air Force Materials Lab., Wright-Patterson AFB, May 1979.

3. Hamilton, C. H., et al.: Superplastic Forming of Titanium Structures. AFML-TR-75-62, Air Force Materials Lab., Wright-Patterson AFB, Apr. 1975. (Primary source - ref. 2).

4. Ko, William L.: Superplastically Formed Diffusion Bonded Metallic Structure. U.S. Patent Appl. 06/043,944, May 30, 1979.

5. Ko, William L.: Elastic Constants for Superplastically Formed/Diffusion-Bonded Sandwich Structures. AIAA Paper 79-0756, Apr. 1979.

6. Ko, William L.: Structural Properties of Superplastically Formed/Diffusion-Bonded Orthogonally Corrugated Core Sandwich Plates. AIAA Paper 80-0304, Jan. 1980.

7. Ko, William L.: Elastic Stability of Superplastically Formed/Diffusion-Bonded Orthogonally Corrugated Core Sandwich Plates. AIAA Paper 80-0683, May 1980.

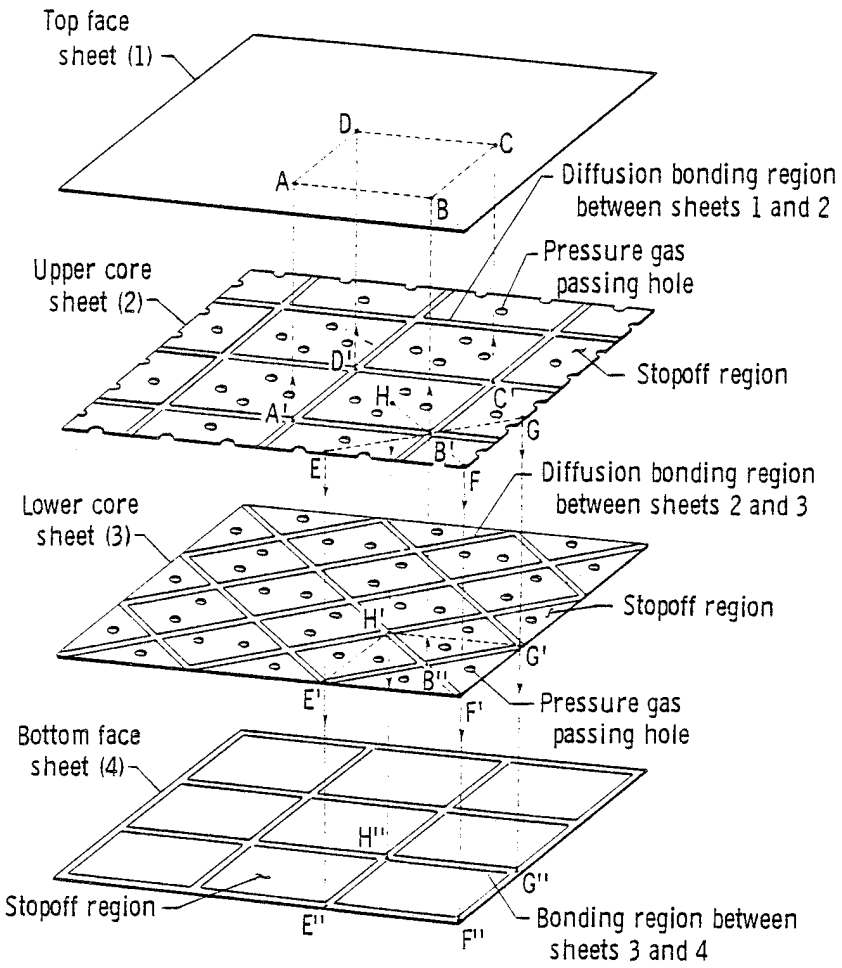

Figure 1. Component sheets for SPF/DB orthogonally corrugated core sandwich panel.

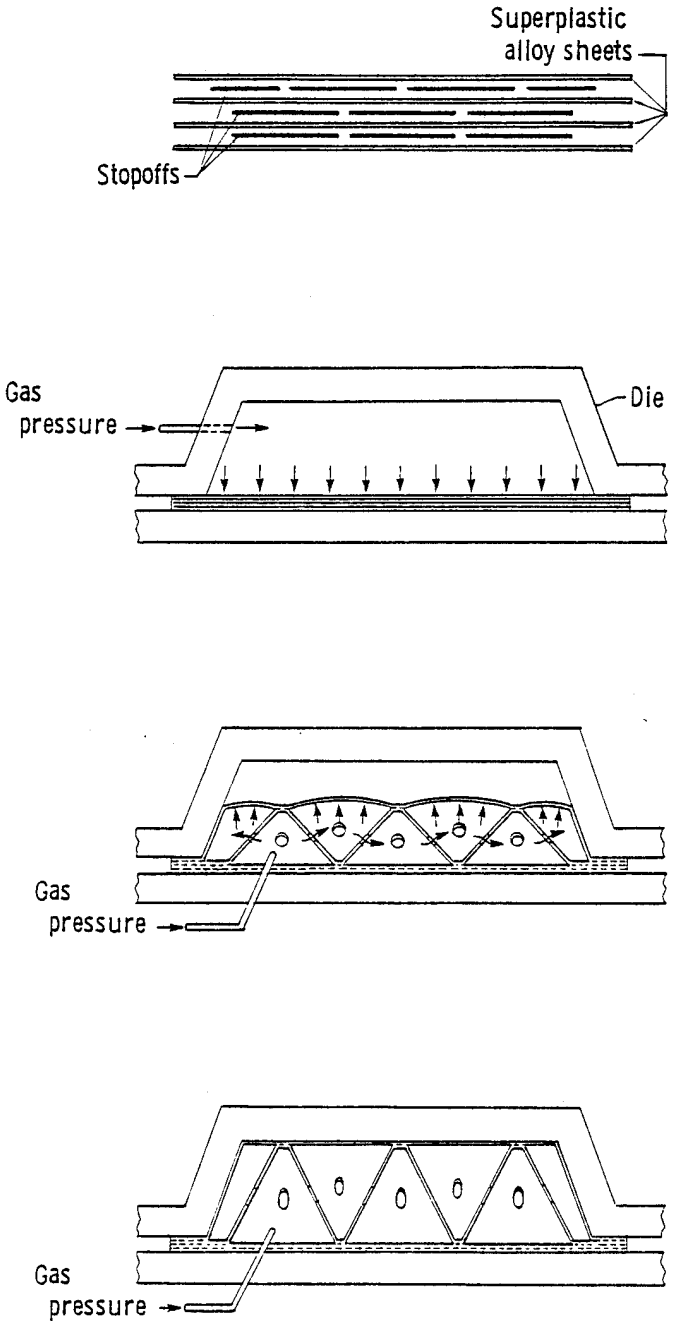

Figure 2. Superplastic forming/diffusion bonding expansion process.

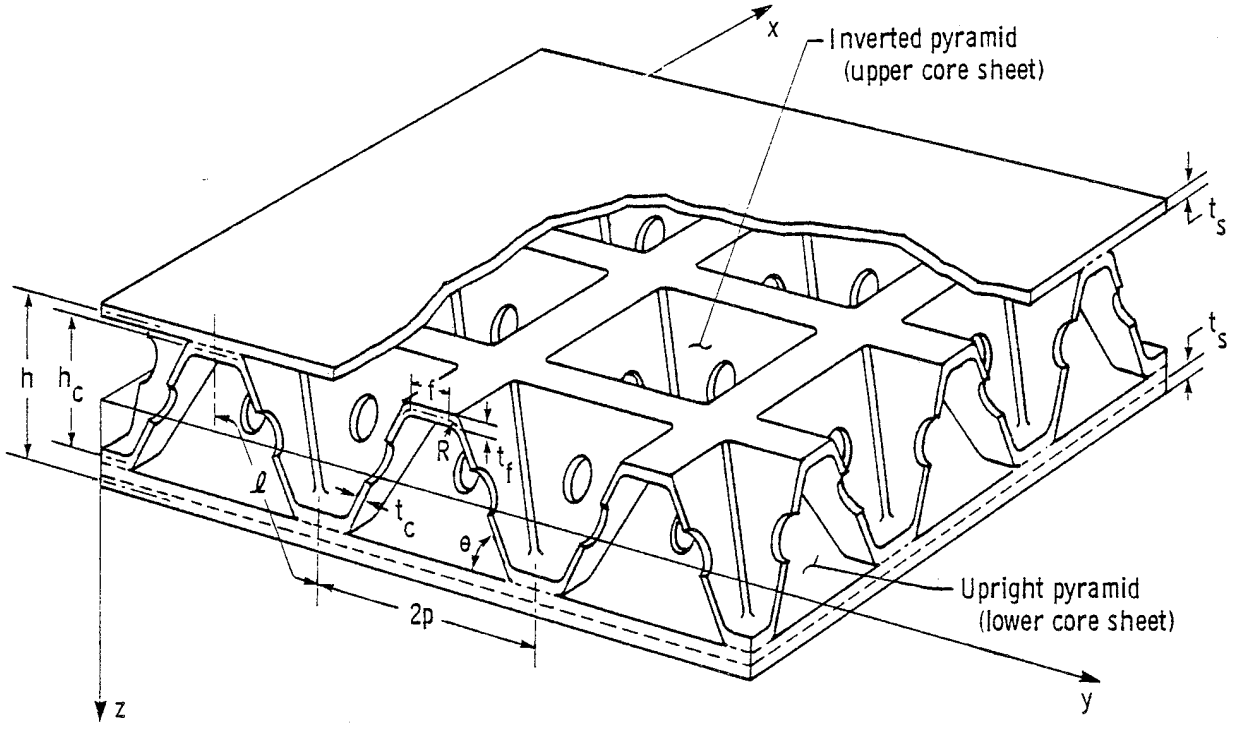

Figure 3. Geometry of SPF/DB orthogonally corrugated core sandwich plate.

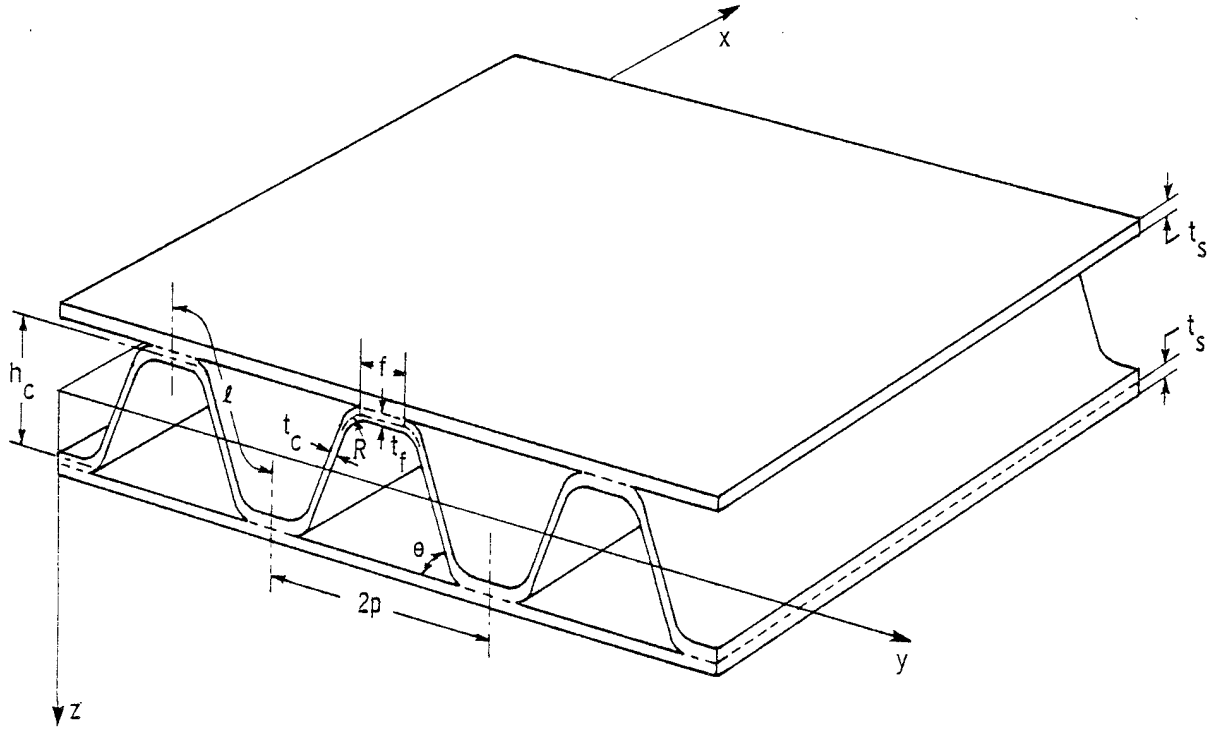

Figure 4. Geometry of SPF/DB unidirectionally corrugated core sandwich plate.

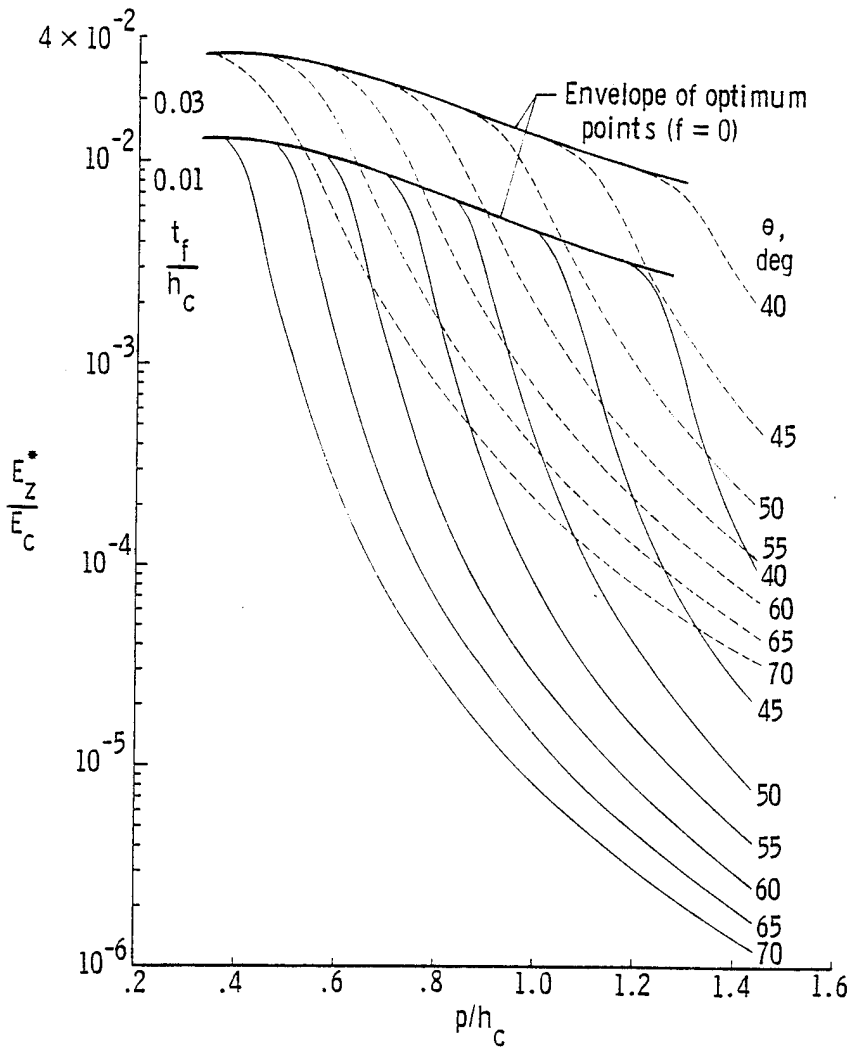

Figure 5. Plots of effective thickness elastic modulus E_z^* for SPF/DB orthogonally corrugated sandwich core. $R = t_f$.

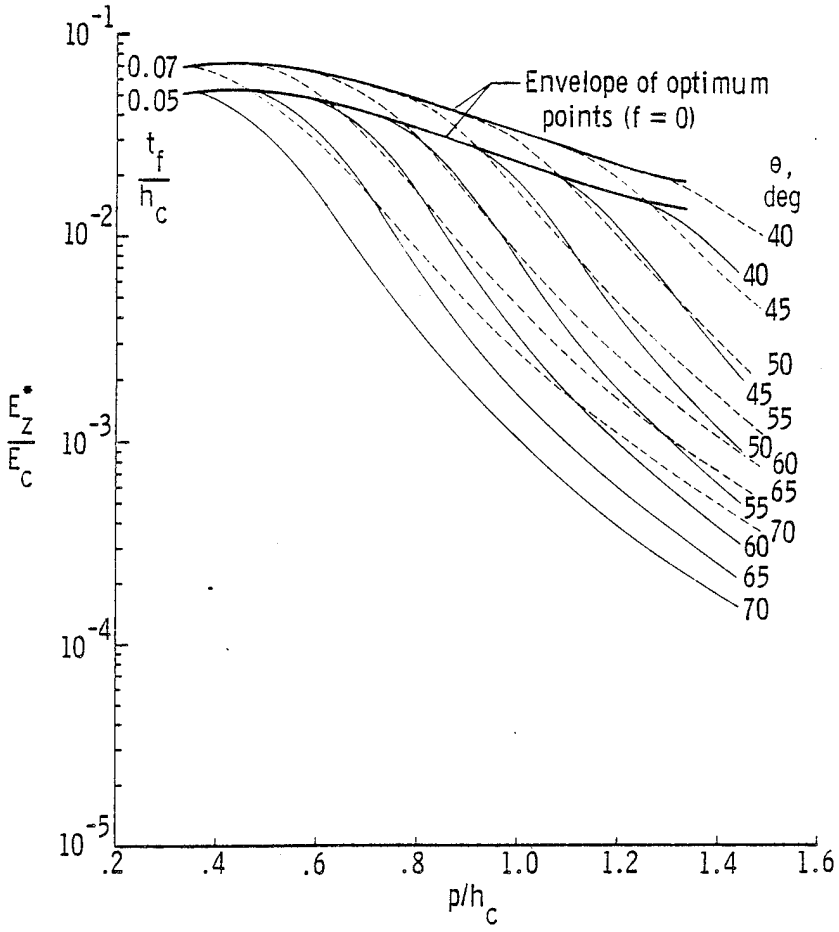

Figure 5. Concluded.

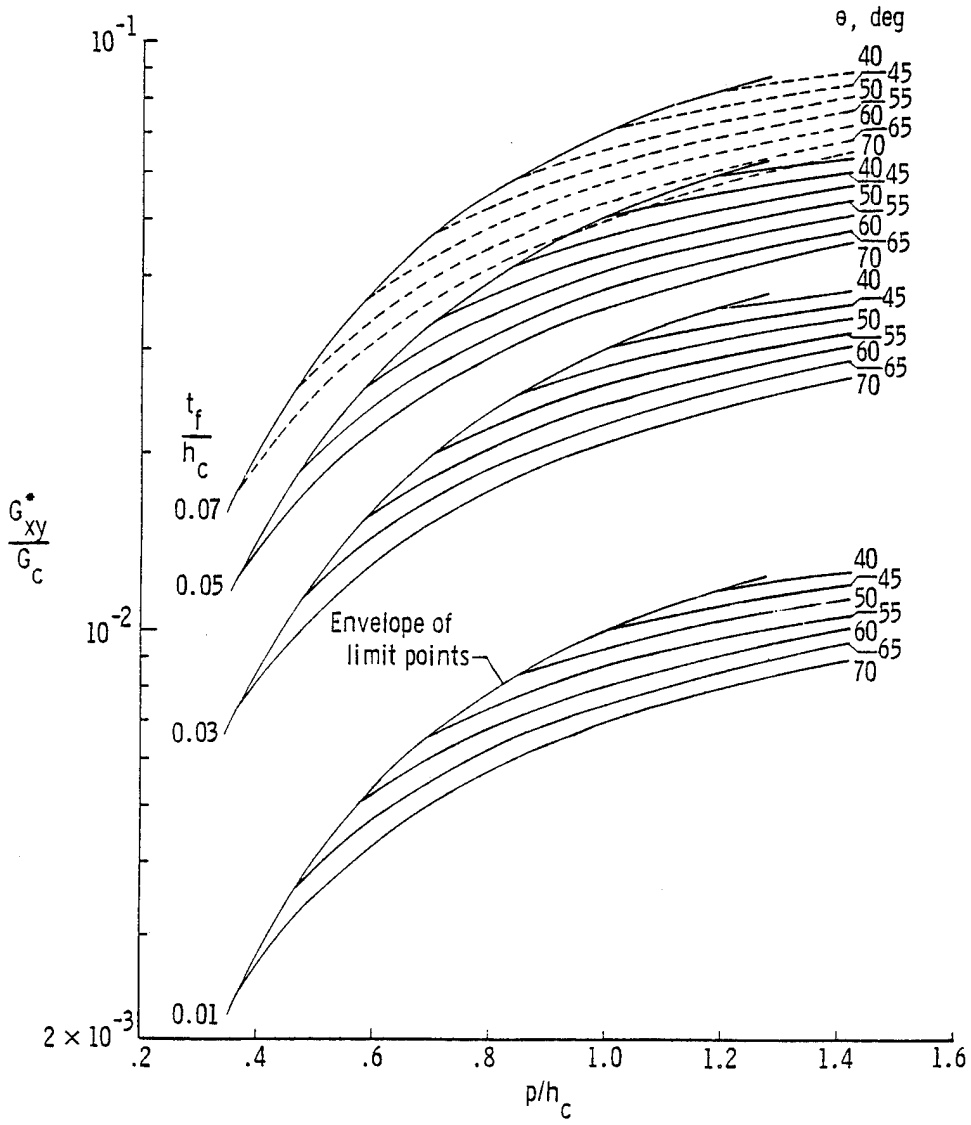

Figure 6. Plots of effective shear modulus G^*_{xy} for SPF/DB orthogonally corrugated sandwich core. $R = t_f$.

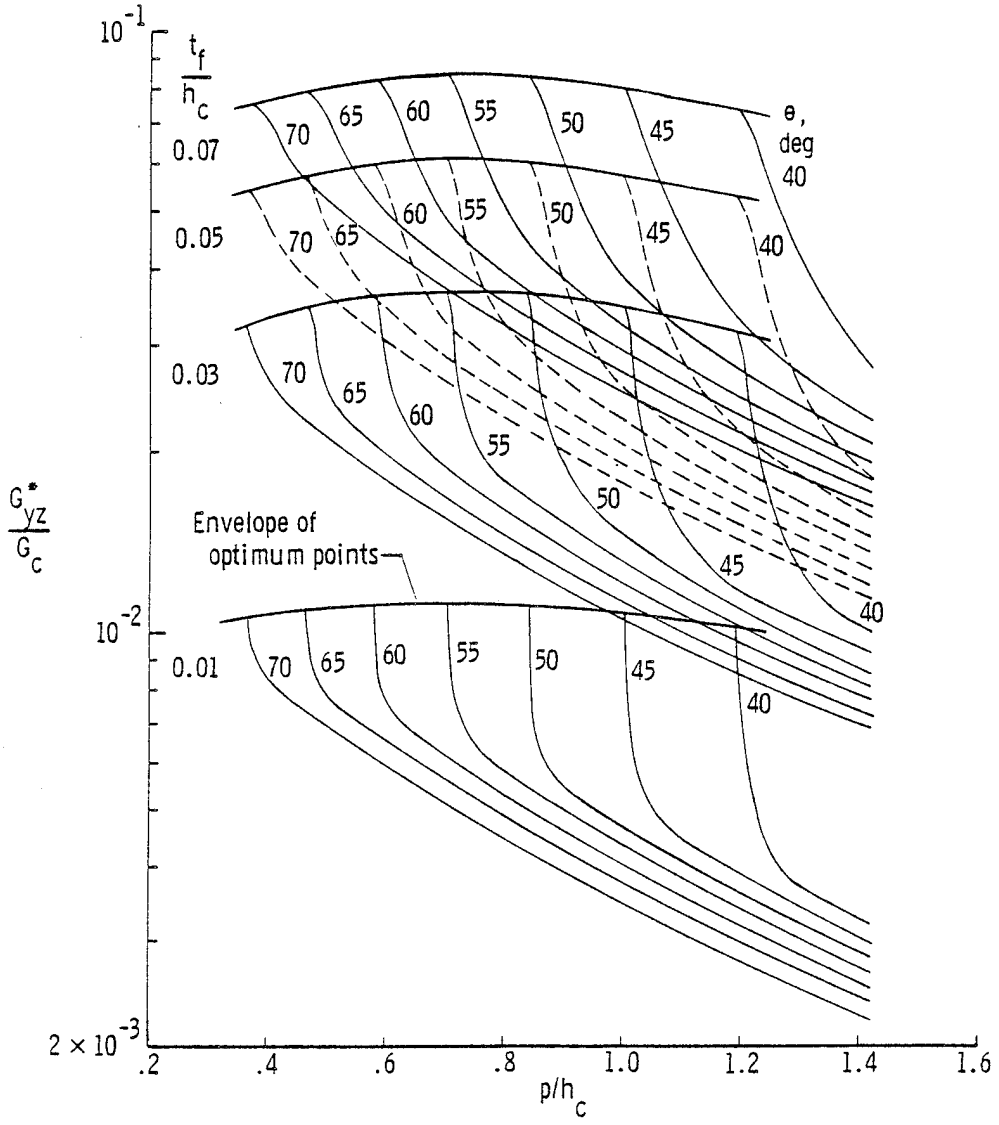

Figure 7. Plots of effective shear modulus G^*_{yz} (= G^*_{zx}) for SPF/DB orthogonally corrugated sandwich core. R = t_f.

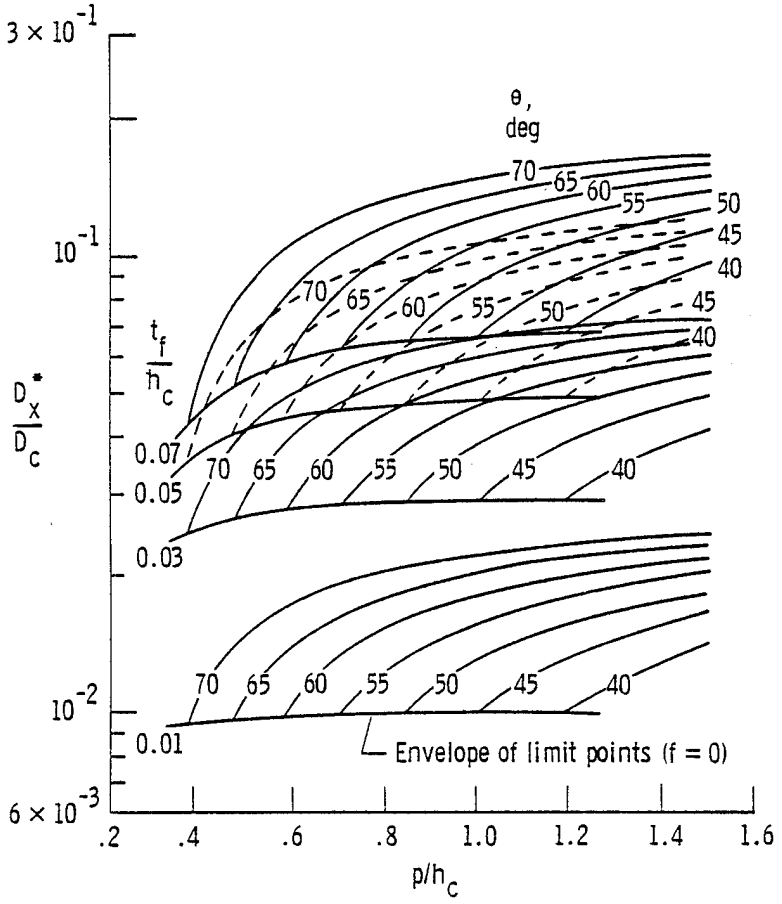

Figure 8. Plots of bending stiffness for SPF/DB orthogonally corrugated sandwich core. $R = t_f$.

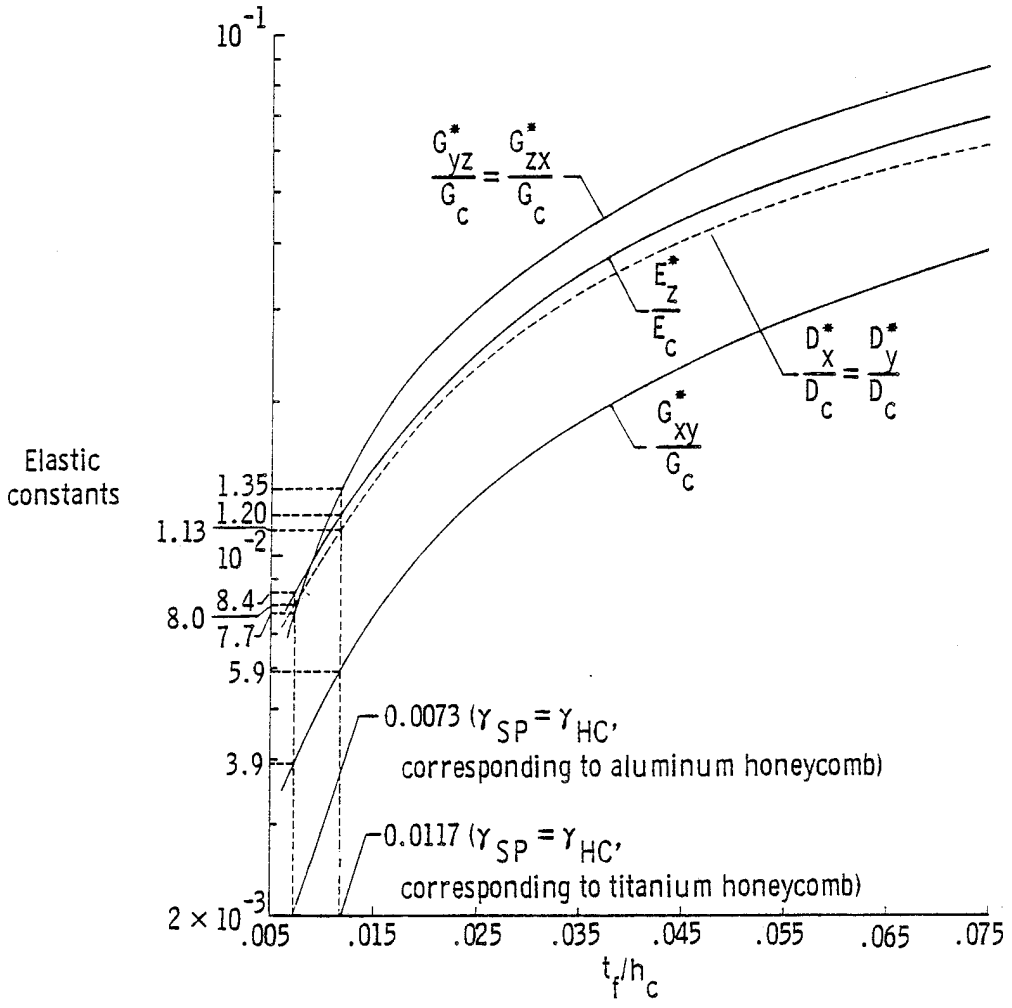

Figure 9. Variation of elastic constants with t_f/h_c for SPF/DB orthogonally corrugated sandwich core. f = 0; θ = 60°; R = t_f.

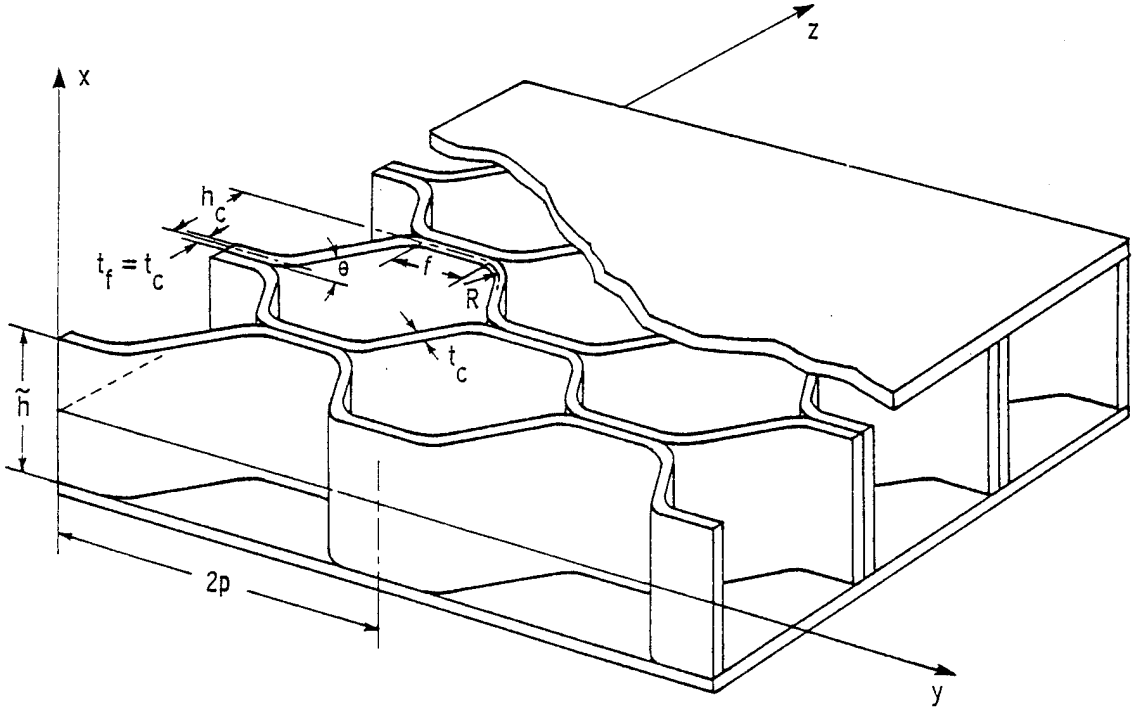

Figure 10. Geometry of honeycomb core sandwich plate.

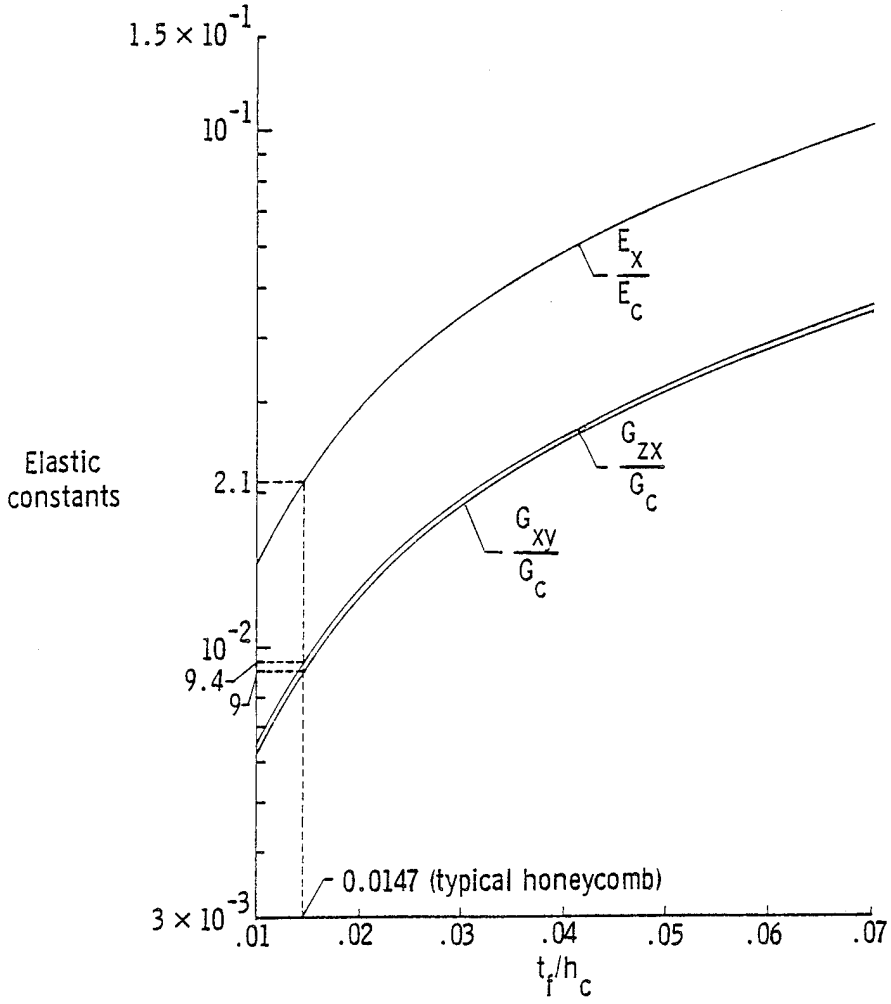

Figure 11. Variation of elastic constants with t_f/h_c for honeycomb sandwich core. $\theta = 60°$; $R = t_c = t_f$; $p/h_c = 0.9825$.

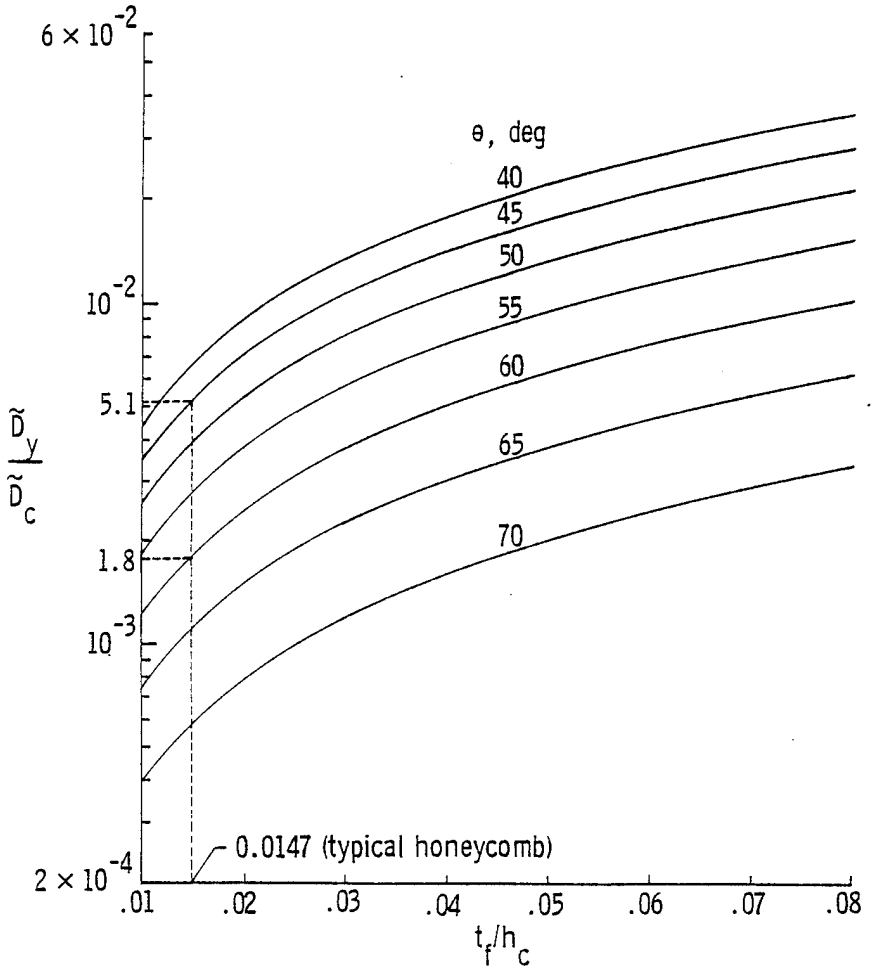

Figure 12. Plots of bending stiffness $\tilde{D}_y$ for honeycomb core. f = 0; $R = t_c = t_f$.

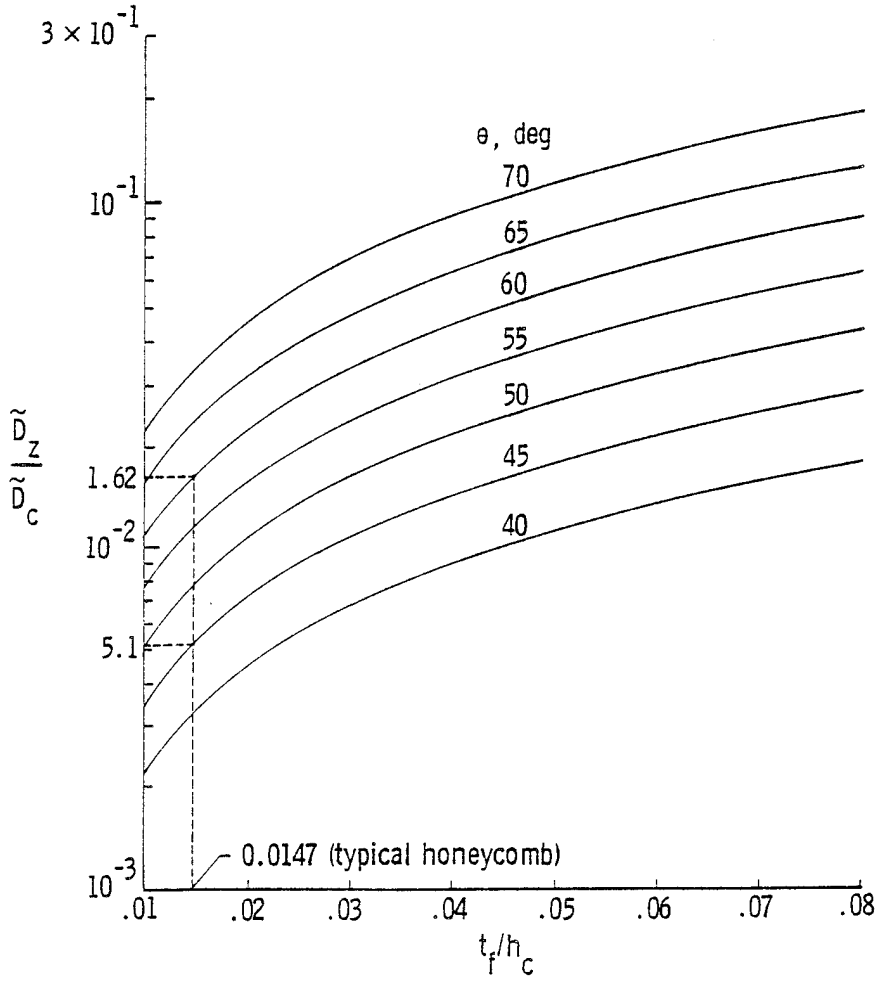

Figure 13. Plots of bending stiffness $\tilde{D}_z$ for honeycomb core. f = 0; $R = t_c = t_f$.

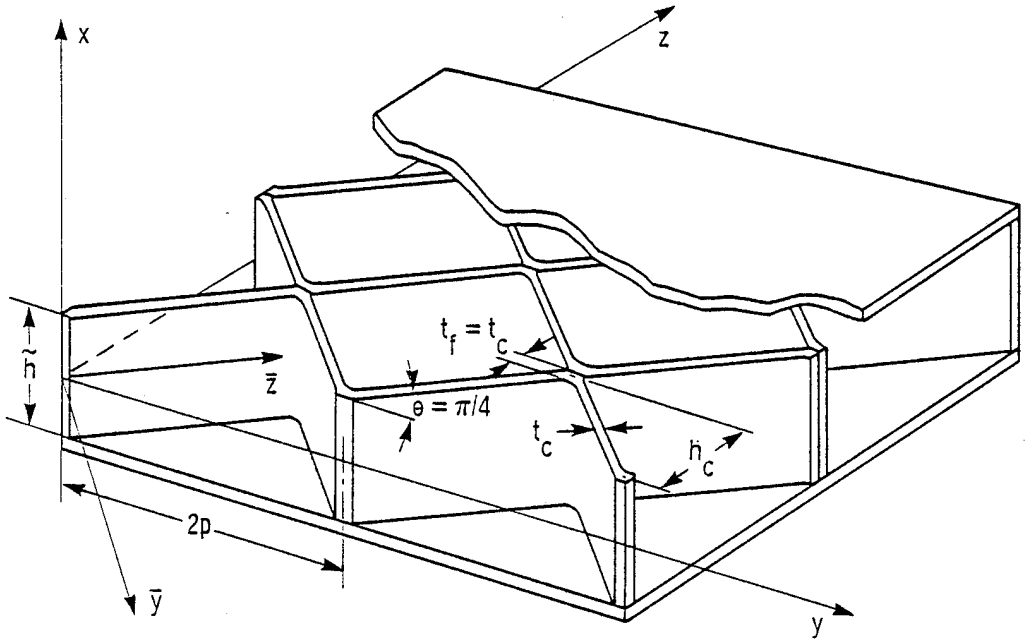

Figure 14. Geometry of square honeycomb core sandwich plate. $f = 0$; $\theta = \pi/4$.

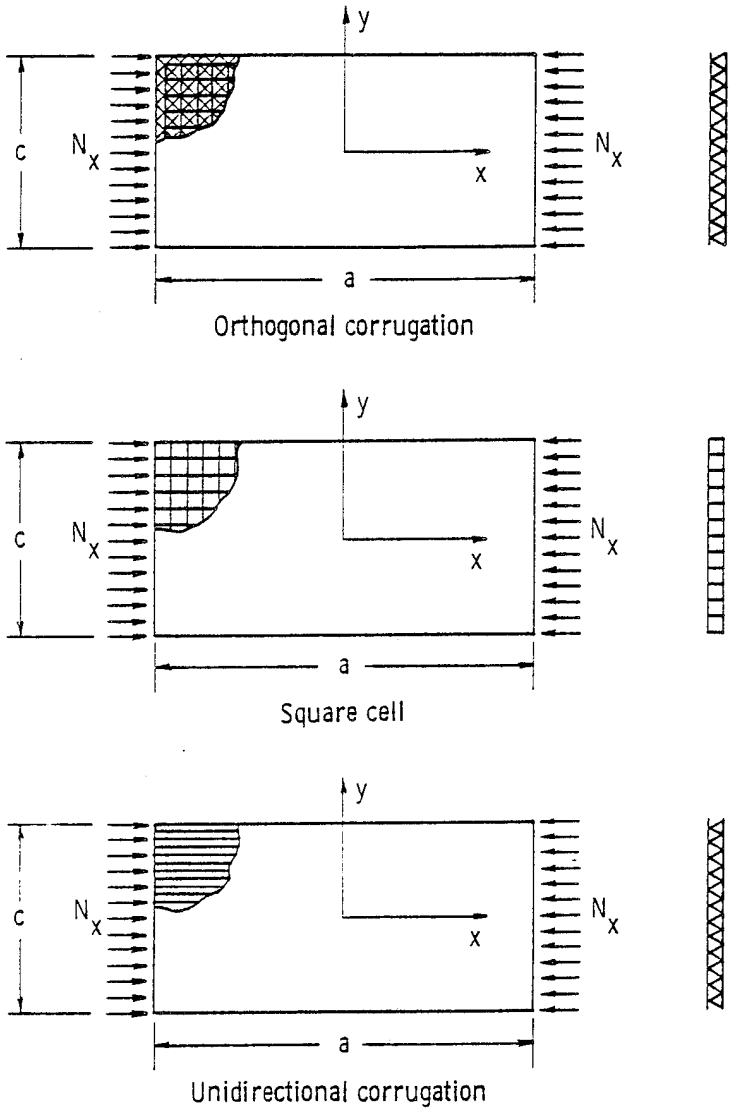

Figure 15. Three types of sandwich plates subjected to edgewise compression (simply supported).

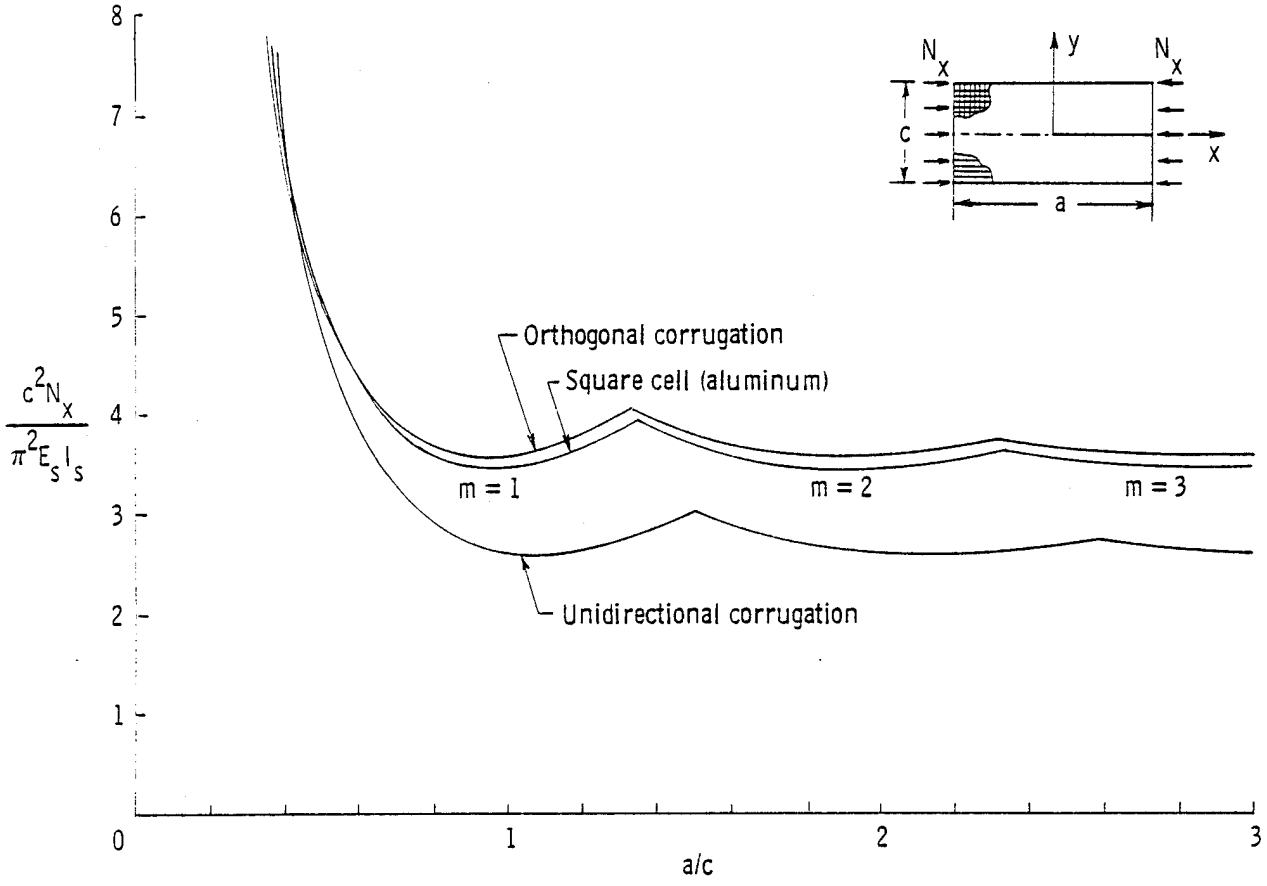

Figure 16. Buckling curves for SPF/DB titanium corrugated core sandwich plates and aluminum square-cell core sandwich plate. For orthogonal corrugation, $t_f/h_c = 0.0073$, $f = 0$, $\theta = 60°$, $t_s/h_c = 0.01$; for unidirectional corrugation, $t_f = 0.0146$, $f = 0$, $\theta = 60°$, $t_s/h_c = 0.01$; for square cell, $t_f/h_c = 0.0165$, $f = 0$, $\theta = 45°$, $t_s/h_c = 0.016$. $E_s = E_c$; $c/h_c = 20$; $\gamma_{SP} = \gamma_{SC}$; $n = 1$.

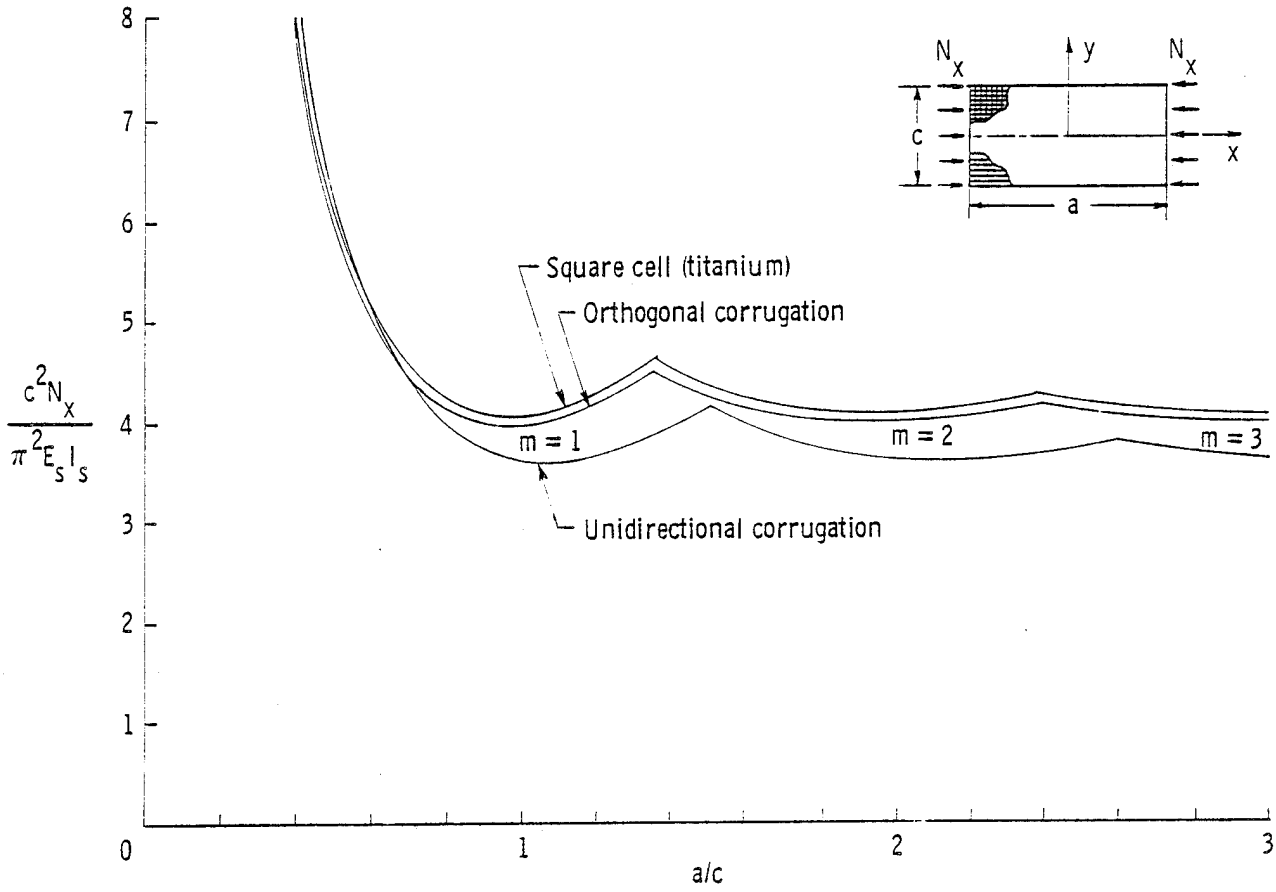

Figure 17. Buckling curves for SPF/DB titanium corrugated core sandwich plates and titanium square-cell core sandwich plate. For orthogonal corrugation, $t_f = 0.0117$, $f = 0$, $\theta = 60°$, and $t_s/h_c = 0.01$; for unidirectional corrugation, $t_f/h_c = 0.0234$, $f = 0$, $\theta = 60°$, $t_s/h_c = 0.01$; for square cell, $t_f/h_c = 0.0165$, $f = 0$, $\theta = 45°$, $t_s/h_c = 0.01$. $E_s = E_c$; $c/h_c = 20$; $\gamma_{SP} = \gamma_{SC}$; $n = 1$.

1. Report No.	2. Government Accession No.	3. Recipient's Catalog No.
NASA TM-81348		

4. Title and Subtitle	5. Report Date
COMPARISON OF STRUCTURAL BEHAVIOR OF SUPER-PLASTICALLY FORMED/DIFFUSION-BONDED SANDWICH STRUCTURES AND HONEYCOMB CORE SANDWICH STRUCTURES	June 1980
	6. Performing Organization Code

7. Author(s)	8. Performing Organization Report No.
William L. Ko	
	10. Work Unit No.

9. Performing Organization Name and Address	11. Contract or Grant No.
NASA Dryden Flight Research Center P. O. Box 273 Edwards, California 93523	
	13. Type of Report and Period Covered
12. Sponsoring Agency Name and Address	Technical Memorandum
National Aeronautics and Space Administration Washington, D. C. 20546	14. Sponsoring Agency Code

15. Supplementary Notes

16. Abstract

This paper discusses a new superplastically formed/diffusion-bonded (SPF/DB) orthogonally corrugated core sandwich structure and compares its structural behavior with that of a conventional honeycomb core sandwich structure.

The stiffness and buckling characteristics of the two types of sandwich structures are compared under conditions of equal structural density.

Under certain conditions, the SPF/DB orthogonally corrugated core sandwich structure is slightly more efficient than the optimum honeycomb core (square-cell core) sandwich structure. However, under different conditions, this effect can be reversed.

17. Key Words (Suggested by Author(s))	18. Distribution Statement
Stiffness Structural properties	Unclassified-Unlimited STAR category: 39

19. Security Classif. (of this report)	20. Security Classif. (of this page)	21. No. of Pages	22. Price*
Unclassified	Unclassified	36	$6.00

*For sale by the National Technical Information Service, Springfield, Virginia 22161